12-1-2001

Influence of Early Lithification on Late Diagenesis of Microbialities: Insights from $\delta^{18}O$ Composition of Upper Cambrian Carbonate Deposits from the Southern Appalachians

B. Glumac
Smith College, bglumac@smith.edu

Influence of Early Lithification on Late Diagenesis of Microbialites: Insights from $\delta^{18}O$ Compositions of Upper Cambrian Carbonate Deposits from the Southern Appalachians

BOSILJKA GLUMAC
Department of Geology, Smith College, Northampton, MA 01063

PALAIOS, 2001, V. 16, p. 593–600

This paper documents a difference in isotopic compositions between Upper Cambrian microbial and non-microbial micritic deposits and proposes implications for diagenesis of calcimicrobial deposits. The $\delta^{18}O$ values (−10.98 to −8.71; average −9.88 ‰ VPDB) of calcimicrite comprising shallow subtidal microbialites from the southern Appalachians are more negative than: (1) the calcimicrite from associated subtidal non-microbial deposits (−8.98 to −7.16; average −7.82), suggesting a different diagenetic history; and (2) estimates of Late Cambrian marine calcite values (−5 to −3 ‰), indicating postdepositional modifications. Early diagenetic calcification of microbial deposits promoted the formation of growth cavities and borings rimmed with marine fibrous and prismatic calcite cement. Some of the voids remained open and provided pathways for fluids during later diagenesis. The microbial deposits, therefore, experienced more pronounced diagenetic alteration than the less porous non-microbial micritic deposits. The $\delta^{18}O$ compositions provided invaluable insights into the influence of early lithification on the later diagenesis of microbialites and into the processes that can result in poor preservation of syndepositional marine isotope signatures in these deposits.

INTRODUCTION

Microbial carbonate deposits are abundant in the rock record and represent an important source of information on local and global biogeochemical processes that operated in the past. Yet it is currently unknown whether and when microbial deposits might preserve syndepositional seawater chemical signals, and which processes influence the preservation of these signals. This paper contributes insights into the importance of evaluating the potential of microbial deposits to preserve syndepositional isotopic signatures, and provides an explanation for some factors that can lead to poor retention of marine isotopic signals.

Glumac and Walker (1997) suggested that subtidal Cambrian calcified microbialites, such as thrombolites and digitate stromatolites, may have good potential for preserving a geochemical signature of syndepositional and early diagenetic conditions. To evaluate the validity of this hypothesis, the current paper presents the results of a stable isotope study of these Cambrian microbial carbonate deposits and associated non-microbial deposits from the southern Appalachians. In particular, this paper: (1) investigates the causes for the differing styles of diagenesis between microbial calcimicrite and associated non-microbial deposits; (2) explores the influence of early diagenesis on the late diagenetic modification of microbialites; and (3) establishes some approaches to identifying and explaining preferential postdepositional alteration of specific types of microbial carbonate deposits.

This study focuses on five outcrops of Upper Cambrian deposits that include the uppermost Nolichucky Shale and the Maynardville Formation (Conasauga Group) and the lower part of the Copper Ridge Dolomite (Knox Group; Fig. 1). These strata crop out within several imbricated, NE–SW trending thrust blocks of the Valley and Ridge province in northeastern Tennessee (Fig. 1). During the Cambrian, this area was a passive continental margin where a large carbonate platform was separated from the exposed craton to the west by the Conasauga intrashelf shale basin. Alternating shale and carbonate deposits of the Conasauga Group were deposited along the western platform margin. These deposits are overlain by peritidal carbonates of the Knox Group that were deposited on a broad carbonate shelf established by platform progradation in a westward direction over the infilled intrashelf basin (Glumac and Walker, 2000).

METHODS

Samples for stable isotope analysis were selected by careful petrographic examination. Special care was exercised to sample homogenous micrite without skeletal fragments, cement, or evidence for extensive recrystallization. Examination of stained thin sections identified areas with non-ferroan, aphanocrystalline to fine-crystalline calcimicrite and fabric retentive dolomicrite to sample, and areas with ferroan microsparite and dolomicrosparite to avoid. Thin sections also were examined using a Citl Cold Cathode Luminescence 8200 mk3 microscope under 10–12 kV voltage, 150–180 μA beam current, and 180–200 millitorr chamber pressure. Areas with a dark, non-luminescent to dark-dull luminescent matrix were sampled. Areas with patchy distribution of bright luminescence and with brightly luminescent crystals scattered in the matrix were avoided. Samples for isotopic analyses were collected by drilling individual carbonate components from polished thin-section billets using a microscope-mounted microdrill. Samples of micritic matrix from microbial deposits and various carbonate cements ranged in size from 2 to 5 mg, whereas samples of dolomicrite (microbial and non-microbial) and non-microbial micrite were as large as 10 mg. Samples for oxygen and carbon isotope analysis were heated at 380°C for 1 hour, reacted with 100% H_3PO_4 at 25°C for 24 hours (calcite) or 48 hours (dolomite), and analyzed on a VG-903 isotope ratio mass spectrometer. Reproducibility of results ($\pm 1\sigma$) was better than 0.2 ‰.

MICROBIAL DEPOSITS

The occurrence and petrography of the Upper Cambrian microbial deposits from the southern Appalachians are described and illustrated in detail in Glumac and Walker (1997). The following sections contain a brief description and interpretation of the origin of these deposits.

0883-1351/01/0016-0593/$3.00

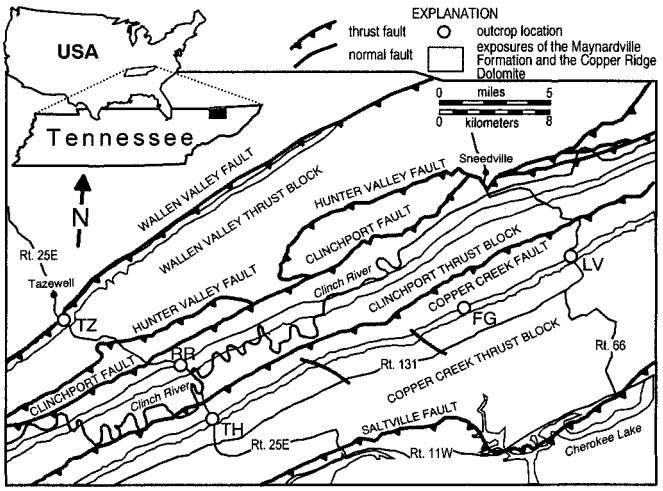

FIGURE 1—Location of outcrops in the southern Appalachians of northeastern Tennessee. Outcrop key: TZ–Tazewell; RR–River Ridge; TH–Thorn Hill; FG–Flat Gap; LV–Lee Valley.

Description

The examined Upper Cambrian strata consist of a lower subtidal and an upper peritidal facies succession (Figs. 2, 3). The subtidal succession contains thrombolitic bioherms, whereas the peritidal succession contains a variety of microbial deposits including: microbial laminites (stratiform stromatolites), domal stromatolites, columnar stromatolites, digitate stromatolites, and thrombolites (Fig. 2).

The subtidal deposits are dominated by ribbon rocks composed of centimeter-scale, alternating limestone and argillaceous layers (shale, siltstone, or silty dolostone; Figs. 2, 3). Samples of non-microbial calcimicrite were collected mainly from the micrite-rich, subtidal limestone layers of ribbon rocks (Fig. 2). The micritic limestone layers commonly are burrow-mottled. Burrows have diffuse walls and are infilled with ferroan microsparite and framboidal pyrite. Intergranular space of subtidal grainstones is occluded by fibrous, prismatic, and equant calcite cements. A gradual vertical change from the ribbon rocks to microbial laminites marks the transition into the peritidal succession (Fig. 2). Peritidal deposits are extensively dolomitized. Centimeter-scale couplets or mechanical laminites with scoured bases, intraclast-, ooid- or peloid-rich lower parts, and micritic tops are the predominant lithofacies (Figs. 2, 3). Samples of dolomicritic matrix came from the couplets, and from the interbedded mudstone layers and microbial deposits (Fig. 2). The most common types of pores in the peritidal deposits are desiccation and evaporite-dissolution voids, and rare burrows occluded with dolomite and equant calcite cements. Microbial deposits also have common fenestrae filled with dolomite cement.

Thrombolites overlie ooid grainstone and flat-pebble conglomerate, and underlie shale and ribbon rocks of the subtidal succession (Fig. 2). In the peritidal succession, thrombolites are interbedded with coarse- to medium-grained couplets, and overlain by digitate stromatolites and other microbial deposits (Fig. 2). Thrombolites comprise bioherms (up to about 1 m thick), characterized by a

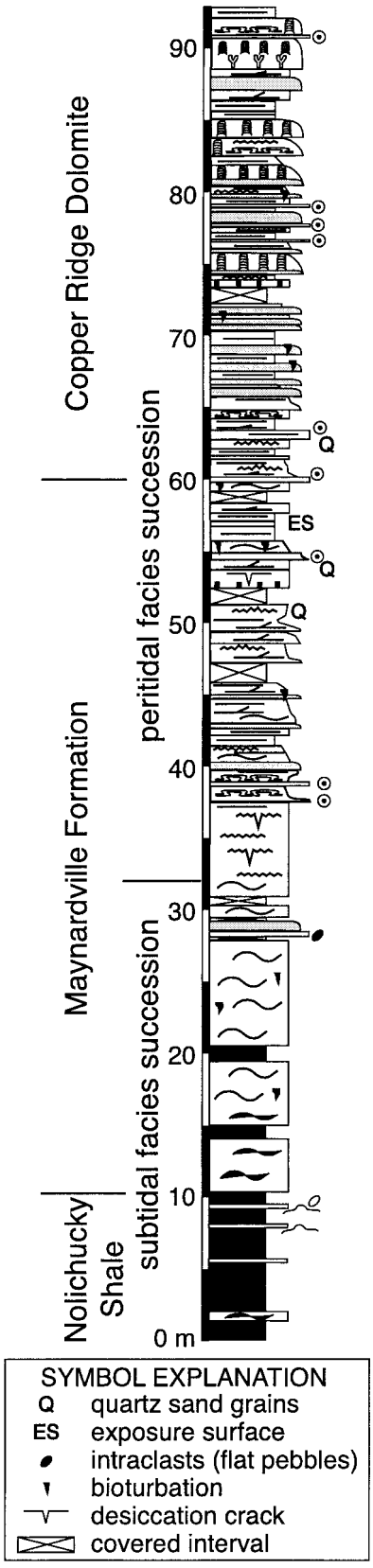

FIGURE 2—Representative stratigraphic column of Upper Cambrian strata measured at the Lee Valley locality. See Figure 1 for outcrop location and Figure 3 for additional symbol explanations.

Subtidal Facies Succession		Symbols and Descriptions	Environments
Thrombolite		microbial bioherms; *Renalcis-Epiphyton-Girvanella* boundstones; borings present.	Shallow subtidal patch reefs
Oolite		ooid- and intraclastic-ooid grainstone; cross-bedding present; rare echinoderm, trilobite, and brachiopod fragments.	Agitated shallow subtidal shoals
Fossiliferous-peloidal packstone/grainstone		common echinoderm and trilobite fragments, intraclasts, pellets, and some ooids; horizontally and cross-laminated.	Moderately agitated shallow subtidal
Ribbon rock	with shale	carbonate layers (skeletal grainstone, peloidal-fossil wacke/packstone, laminated and burrowed mudstone) alternating with siltstone and shale.	Storm-dominated shallow ramp
	without shale	carbonate layers (burrow-mottled mudstone, peloidal packstone) alternating with argillaceous dolostone and calcareous siltstone.	Protected lagoon
Shale		silty shale and calcareous siltstone; in places contains thin limestone layers compositionally similar to limestone from the ribbon rock.	Shallow to deep ramp

Peritidal Facies Succession		Symbols and Descriptions	Environments
Couplets	Coarse-grained	intraclastic packstone/grainstone (+/- ooids, quartz sand and silt), grading upward into peloidal packstone and mudstone.	Agitated shallow subtidal to intertidal
	Medium-grained	horizontally and cross-laminated peloidal packstone/grainstone (+/- small intraclasts, ooids, quartz silt), grading upward into mudstone.	
	Fine-grained	thin basal laminae/lenses of peloidal packstone overlain by dolomicrite with desiccation cracks and evaporite molds.	Less agitated upper intertidal to supratidal
Dolomitized mudstone		massive dolomicrite; some horizontal lamination, mottling (burrows?), desiccation cracks, subaerial exposure surfaces and evaporite molds.	
Calcareous siltstone		thinly bedded; horizontally and cross-laminated; desiccation cracks, microbial laminae, fenestrae, and peloids present; interbedded with silty calcareous shale.	Moderately agitated intertidal
Oolite		ooid grainstone; single layers of variable thickness or composite bodies of several layers; ooid packstones at bases of coarse-grained couplets.	Small localized high energy ooid shoals
Microbial deposits	Thrombolite	bioherms with clotted fabric; irregular to digitate and branching patches of dense micrite; *Renalcis* present; common borings.	Agitated shallow subtidal
	Digitate stromatolite	bioherms composed of branching columns of low relief; crudely laminated micritic pelleted fabric; borings present.	
	Columnar stromatolite	laminated, non-linked, vertically stacked columns of cylindrical or club shape; desiccation cracks and fenestrae present.	Agitated to protected intertidal
	Domal stromatolite	hemispheroids composed of wavy laminated micrite; small desiccation cracks and fenestrae present.	
	Microbial laminites	micritic laminae with lenses of pellets/peloids, ooids, and quartz silt; common desiccation cracks, fenestrae, and evaporite molds.	Restricted upper intertidal to supratidal

FIGURE 3—A summary of characteristic features and environmental interpretations for the lithofacies present. Symbols correspond to those in Figure 2.

clotted fabric made up of patches or mesoclots of dark, dense micrite. Some mesoclots have well-preserved calcimicrobial forms of *Renalcis, Epiphyton,* and *Girvanella* (Glumac and Walker, 1997). Thrombolites contain growth cavities (Fig. 4A) and borings (Fig. 4B). These voids are floored with geopetal sediment, rimmed with fibrous and prismatic calcite cement, and occluded with equant calcite. Thrombolites also have voids of uncertain origin (dissolution-enlarged?) occluded with equant calcite (Fig. 4C) and rare pore-central saddle dolomite. Digitate stromatolites form bioherms and biostromes (up to 1.5 m thick) that are characterized by branching columns of low relief composed of crudely laminated, micritic, pelleted (clotted) fabric, and are surrounded by ooid-peloidal packstone/grainstone. Digitate stromatolites and thrombolites have similar types of pores and occluding cements (Fig. 4), and compose the rare lithofacies in the peritidal succession that were not extensively dolomitized, even though they are interbedded with completely dolomitized deposits (Glumac and Walker, 1997).

Origin

The patterns of selective dolomitization of microbial deposits and their association with non-microbial deposits correlate with microbialite origin (Glumac and Walker, 1997). Pervasively dolomitized columnar, domal, and stratiform stromatolites formed by the trapping of particles in restricted intertidal and supratidal environments of a semiarid tidal flat (Fig. 3), as indicated by the presence of desiccation cracks, evaporite-mineral pseudomorphs, and the similarity with modern agglutinated stromatolites (Logan et al., 1974; Playford and Cockbain, 1976). The absence of preserved cyanobacterial forms suggests that calcification of cyanobacteria was not prominent during the formation of these deposits. In the absence of processes that promote early calcification, micrite trapped on microbial substrates was susceptible to early diagenetic dolomitization. In contrast, non-dolomitized digitate stromatolites and thrombolites formed broad, low-relief mounds in less restricted, agitated, shallow subtidal environments (Fig. 3). This is sup-

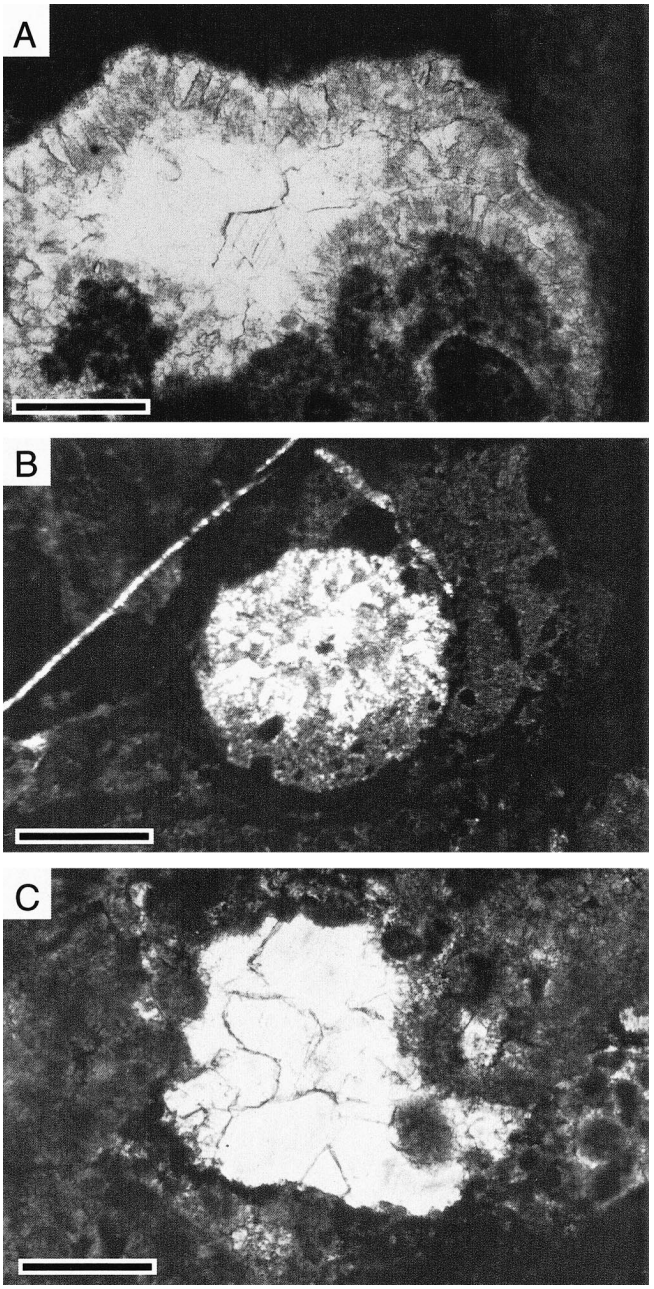

FIGURE 4—Plain-light photomicrographs of common types of pores and occluding cement in thrombolites and digitate stromatolites. (A) Microbial deposit with a growth cavity rimmed with turbid fibrous calcite cement and occluded with less turbid equant calcite. Scale bar = 0.5 mm. (B) Boring filled with geopetal sediment and turbid fibrous to prismatic calcite cement. Scale bar = 1 mm. (C) Void of uncertain origin (dissolution-enlarged?) occluded with equant calcite cement. Scale bar = 0.5 mm.

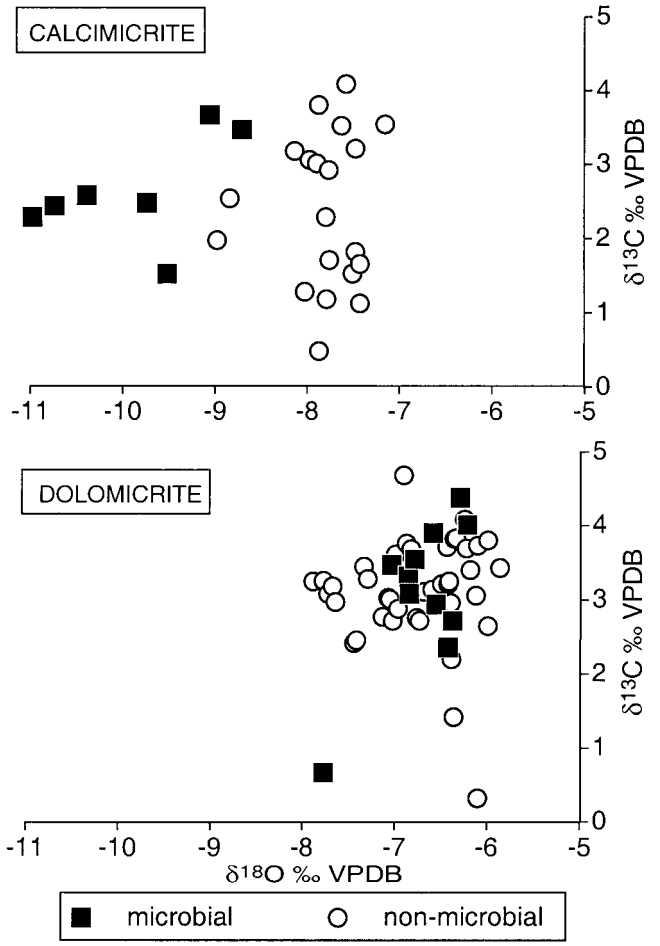

FIGURE 5—Comparison of stable isotope compositions of microbial and non-microbial calcimicrite and dolomicrite.

ported by the absence of exposure indicators, the presence of bioturbation, and the association with skeletal fragments, ooids, peloids, and intraclasts. The fact that digitate stromatolites and thrombolites commonly are surrounded by completely dolomitized deposits suggests that early lithification of these microbial deposits may have reduced their susceptibility to dolomitization (Glumac and Walker, 1997). Early diagenetic lithification of these microbial deposits may have been promoted, in part, by calcification of cyanobacteria, as suggested by the presence of *Renalcis, Epiphyton,* and *Girvanella* (Riding, 1975; Pratt, 1984; Kennard and James, 1986). Calcification also may have been related to heterothrophic bacterial decomposition and sulfate-reducing processes (Chafetz and Buczynski, 1992; Visscher et al., 1998; Reid et al., 2000; Riding, 2000). The absence of coarse-grained agglutinated particles within microbial "digits" and mesoclots substantiates the formation of digitate stromatolites and thrombolites through calcification by cyanobacteria and bacteria. Early lithification of thrombolites and digitate stromatolites is further indicated by well-preserved borings and growth cavities rimmed with marine fibrous and prismatic calcite cements (Fig. 4A,B).

ISOTOPIC COMPOSITIONS OF MICROBIAL DEPOSITS

Observations

The $\delta^{18}O$ compositions of dolomicrite from the peritidal microbial deposits that formed by sediment trapping (-7.77 to -6.21; average -6.70 ‰ VPDB) are similar to dolomicrite from the associated non-microbial deposits (-7.88 to -5.86; average -6.72; Fig. 5; Table 1). In contrast, the $\delta^{18}O$ values of calcimicrite from the shallow sub-

TABLE 1—Stable isotope data for dolomicritic matrix samples.

Locality	Source	‰ VPDB $\delta^{18}O$	‰ VPDB $\delta^{13}C$
Dolomicritic matrix of microbial deposits			
TZ	Stratiform stromatolite	−6.29	4.38
TH	Stratiform stromatolite	−6.58	3.90
TH	Stratiform stromatolite	−6.21	4.01
TH	Domal stromatolite	−6.78	3.55
TH	Domal stromatolite	−6.55	2.94
TH	Stratiform stromatolite	−6.37	2.72
TH	Domal stromatolite	−6.42	2.36
TH	Domal stromatolite	−7.77	0.67
FG	Stratiform stromatolite	−6.85	3.32
FG	Domal stromatolite	−6.84	3.08
LV	Stratiform stromatolite	−7.03	3.47
Dolomicritic matrix of non-microbial deposits			
TZ	Fine-grained couplets	−6.73	2.72
TZ	Fine-grained couplets	−6.22	3.69
TH	Dolomitized mudstone	−6.41	3.25
TH	Coarse-grained couplets	−6.76	2.76
TH	Fine-grained couplets	−7.02	2.72
TH	Fine-grained couplets	−7.41	2.46
TH	Fine- to medium-grained couplets	−7.07	3.03
TH	Fine-grained couplets	−7.05	3.01
TH	Dolomitized mudstone	−7.88	3.25
TH	Dolomitized mudstone	−7.29	3.28
TH	Dolomicritic intraclast	−7.77	3.25
TH	Dolomicritic intraclast	−7.67	3.18
TH	Fine-grained couplets	−7.72	3.08
TH	Dolomitized mudstone	−6.82	3.68
TH	Dolomitized mudstone/fine couplets	−6.12	3.06
TH	Medium-grained couplets	−6.96	2.88
TH	Fine- to medium-grained couplets	−6.39	2.96
TH	Dolomitized mudstone	−6.59	3.14
TH	Fine- to medium-grained couplets	−5.86	3.43
TH	Medium-grained couplets	−6.35	3.82
TH	Medium-grained couplets	−5.99	3.80
TH	Medium-grained couplets	−6.99	3.61
TH	Mudstone to fine-grained couplets	−6.87	3.76
TH	Fine-grained couplets to mudstone	−6.18	3.40
TH	Mudstone to fine-grained couplets	−6.24	4.08
TH	Fine-grained couplets	−6.33	3.83
TH	Fine-grained couplets	−6.68	3.11
TH	Coarse-grained couplets	−5.99	2.65
TH	Fine-grained couplets	−6.38	2.20
TH	Fine-grained couplets	−7.44	2.42
TH	Mudstone to fine-grained couplets	−6.43	3.71
TH	Fine- to medium-grained couplets	−7.13	2.77
TH	Fine-grained couplets	−6.36	1.42
TH	Burrowed fine-grained couplets	−6.10	0.32
FG	Dolomitized mudstone	−7.33	3.45
FG	Dolomitized mudstone	−6.42	3.21
FG	Dolomitized mudstone	−6.49	3.21
LV	Medium- to coarse-grained couplets	−6.10	3.73

TABLE 2—Stable isotope data for calcimicritic matrix samples.

Locality	Source	‰ VPDB $\delta^{18}O$	‰ VPDB $\delta^{13}C$
Calcimicritic matrix of microbial deposits			
TZ	Thrombolitic mesoclots	−9.06	3.67
TZ	Thrombolitic mesoclots	−8.71	3.47
RR	Thrombolite to digitate stromatolite	−10.74	2.44
RR	Digitate stromatolite	−10.98	2.29
TH	Digitate stromatolite	−9.52	1.53
FG	Digitate stromatolite	−10.39	2.58
FG	Digitate stromatolite	−9.74	2.48
Calcimicritic matrix of non-microbial deposits			
TH	Ribbon rock (intraclasts)	−8.98	1.98
TH	Ribbon rock (mudstone)	−8.84	2.54
TH	Ribbon rock (burrowed mudstone)	−7.90	3.01
TH	Ribbon rock (laminated mudstone)	−7.48	1.82
TH	Ribbon rock (mudstone)	−7.43	1.66
TH	Ribbon rock (packstone)	−8.03	1.29
TH	Ribbon rock (intraclasts)	−7.87	0.49
TH	Ribbon rock (mudstone)	−7.79	1.19
TH	Ribbon rock (peloidal mudstone)	−7.51	1.53
TH	Ribbon rock (wackestone/packstone)	−7.43	1.13
TH	Ribbon rock (mudstone)	−7.77	2.92
TH	Ribbon rock (mudstone)	−7.76	1.71
TH	Ribbon rock (peloidal mudstone)	−8.14	3.18
TH	Ribbon rock (mudstone)	−7.48	3.21
TH	Ribbon rock (mudstone)	−7.16	3.54
TH	Ribbon rock (mudstone)	−7.58	4.09
TH	Ribbon rock (mudstone)	−7.80	2.29
TH	Ribbon rock (mudstone/packstone)	−7.63	3.52
TH	Ribbon rock (burrowed mudstone)	−7.88	3.80
FG	Ribbon rock (mudstone)	−7.98	3.06

tidal microbial deposits that formed by cyanobacterial and bacterial calcification (−10.98 to −8.71; average −9.88) are more negative than calcimicrite from the non-microbial deposits (−8.98 to −7.16; average −7.82; Fig. 5; Table 2), and estimates for Late Cambrian marine calcites (−5 to −3 ‰; Lohmann and Walker, 1989; Gao and Land, 1991). The $\delta^{18}O$ values of microbial calcimicrite overlap with fibrous to prismatic (−10.16 to −7.48; average −8.92), equant (−10.65 to −8.83; average −9.53), ferroan equant (−11.00 to −9.07; average −9.87), and fracture-occluding equant calcite cements (−12.92 to −9.38; average −11.22; Fig. 6; Table 3). The $\delta^{13}C$ values of the microbial deposits (0.67 to 4.38 ‰ VPDB) and all other components vary greatly (Figs. 5, 6; Tables 1–3).

Interpretations and Implications

A wide range of determined $\delta^{13}C$ compositions reflects a short-term secular increase in the $^{13}C/^{12}C$ ratio of Late Cambrian (Steptoean) seawater by 4–5‰ (Glumac and Walker, 1998). The secular nature of this excursion is confirmed by studies of coeval successions in the Great Basin, Kazakhstan, and China (Brasier, 1993; Saltzman et al., 1998). The $\delta^{13}C$ values of individual samples depend mainly on the stratigraphic position of the sample, with possible effects of variations in environmental conditions and diagenesis in the presence of degrading organic matter (e.g., Patterson and Walter, 1994; Andrews et al., 1997) superimposed on the secular marine $^{13}C/^{12}C$ trend (Glumac and Walker, 1998).

All calcimicritic samples have $\delta^{18}O$ compositions at least 3 to 4 ‰ more negative than estimated Late Cambrian marine calcite, with the $\delta^{18}O$ values of microbial micrite being more negative than those of non-microbial micrite (Fig. 5). These observations could reflect: (1) temperature or salinity variations within the environment of deposition; (2) formation of microbial deposits by non-equilibrium precipitation due to vital effects; or (3) a greater degree of diagenetic modification of microbial deposits with re-

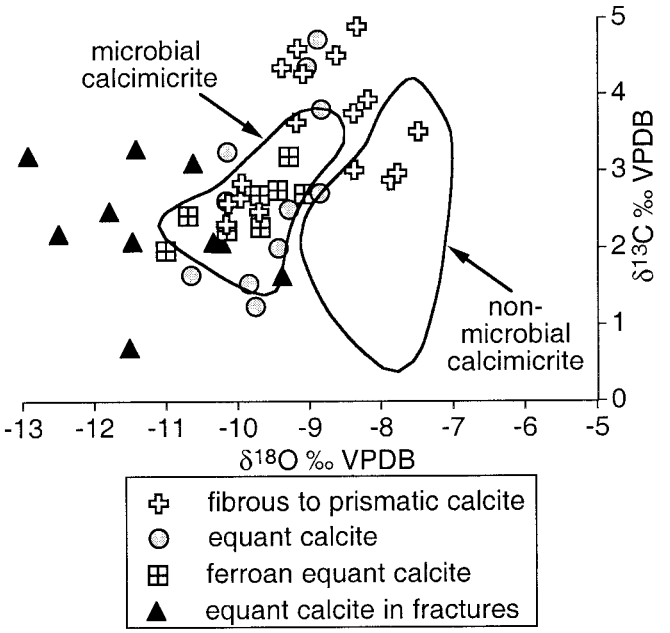

FIGURE 6—Comparison of stable isotope compositions of microbial and non-microbial calcimicrite with carbonate cements (compositional fields from data on Fig. 5).

spect to non-microbial deposits. Calcimicritic microbial and non-microbial deposits most likely formed under a similar temperature and salinity regime because these deposits formed in similar shallow subtidal settings where microbes were forming low-relief mounds (Glumac and Walker, 1997). The presence of calcified thrombolites and digitate stromatolites interbedded with dolomitized peritidal deposits with common evaporite-mineral pseudomorphs suggests that the diagenesis of these microbial deposits may have been influenced by hypersaline fluids. If this were the case, the compositions of these microbial deposits would be relatively enriched in ^{18}O rather than depleted (Fig. 5). Thus, temperature and salinity variations within the depositional environment cannot account for the observed differences in $\delta^{18}O$ values (Fig. 5). Comparisons between microbial deposits and marine cements by other researchers suggest that there are no measurable vital effects in Proterozoic and Lower Cambrian microbial deposits, and that Cambrian calcimicrobes precipitated carbonate in equilibrium with ambient seawater in the absence of vital effects (Fairchild et al., 1990; Surge et al., 1997). Therefore, diagenetic alteration is the most plausible explanation for the observed $\delta^{18}O$ values.

Early diagenetic calcification enhanced the formation and preservation of growth cavities and borings in microbial calcimicritic deposits (Fig. 4A,B). The pores that were not occluded completely during early marine diagenesis provided pathways for the migration of fluids during later diagenesis. This is suggested by non-marine equant calcite cement in the centers of larger pores (Fig. 4A), by dissolution modification and occlusion of pores with equant calcite (Fig. 4C), and saddle dolomite cements of burial origin. The $\delta^{18}O$ values of shallow subtidal microbial calcimicrite reflect diagenetic alteration by: (1) meteoric waters during subaerial exposure of overlying peritidal deposits (Fig. 2); and/or (2) burial fluids at elevated temperature—

TABLE 3—Stable isotope data for calcite cement samples.

Locality	Source (lithology; porosity type)	‰ VPDB $\delta^{18}O$	‰ VPDB $\delta^{13}C$
Fibrous to prismatic calcite cement			
TZ	Ribbon rock; intergranular	−8.62	4.51
TZ	Ribbon rock; intergranular	−8.33	4.89
TZ	Peloidal grainstone; intergranular	−9.16	4.60
TZ	Peloidal pack/grainstone; burrows	−9.38	4.35
TZ	Peloidal pack/grainstone; intergranular	−9.08	4.27
TZ	Peloidal pack/grainstone; burrows	−8.18	3.93
RR	Thrombolite; framework	−8.37	3.01
RR	Thrombolite; borings	−10.13	2.58
RR	Thrombolite; borings	−9.94	2.84
RR	Thrombolite; borings	−9.18	3.63
RR	Thrombolite; borings	−8.38	3.75
RR	Thrombolite; borings	−9.70	2.47
TH	Flat pebble conglomerate; intergranular	−7.86	2.88
TH	Flat pebble conglomerate; intergranular	−7.77	2.97
TH	Coarse-grained couplets; intergranular	−9.96	2.65
FG	Grainstone; intergranular and shelter	−10.16	2.31
LV	Intraclast-peloid grainstone; intergran.	−7.48	3.51
Equant calcite cement			
TZ	Ribbon rock; intergranular	−10.16	2.61
TZ	Ribbon rock; intergranular	−8.88	4.72
TZ	Stratiform stromatolite; burrows	−8.83	3.80
TZ	Peloidal pack/grainstone; dissolution	−9.03	4.36
TZ	Peloidal pack/grainstone; burrows	−10.14	3.25
RR	Thrombolite; borings	−9.75	1.24
TH	Digitate stromatolite; framework	−9.84	1.54
FG	Ribbon rock; burrow(?)/synaeresis(?)	−8.85	2.71
FG	Mechanical couplets; burrows	−10.65	1.65
FG	Thrombolite; borings	−9.28	2.50
LV	Thrombolite; borings	−9.43	2.00
Ferroan equant calcite cement			
TZ	Grainstone; burrows	−10.69	2.42
RR	Stratiform stromatolite; burrows	−9.28	3.19
RR	Thrombolite; framework	−9.44	2.75
TH	Ribbon rock; burrow(?)	−9.68	2.27
TH	Ribbon rock; burrow(?)	−9.07	2.70
TH	Stratiform stromatolite; burrows	−9.69	2.69
FG	Couplets; burrows	−11.00	1.97
FG	Thrombolite; borings	−10.15	2.23
Equant calcite cement in fractures (F = ferroan)			
TZ	Thrombolite (F)	−12.92	3.20
RR	Ribbon rock (F)	−11.79	2.48
RR	Skeletal packstone/grainstone (F)	−10.23	2.07
RR	Ribbon rock (F)	−11.47	2.09
RR	Fine-grained couplets to mudstone	−10.34	2.08
RR	Extensively deformed layer	−11.51	0.70
RR	Stratiform stromatolite	−11.42	3.29
RR	Stratiform stromatolite (F)	−10.62	3.10
FG	Dolomitized mudstone (F)	−12.50	2.19
LV	Ribbon rock (F)	−9.38	1.64

the Upper Cambrian deposits from the study area were buried to a depth of about 4.5 km (Glumac, 1997). The $\delta^{18}O$ composition of microbial calcimicrite overlaps with: (1) fibrous and prismatic calcite cements that are morphologically similar to documented occurrences of marine cement, but have $\delta^{18}O$ compositions indicative of diagenetic modifications; (2) equant calcite cements interpreted to represent meteoric to burial diagenesis; and (3) fracture-occluding equant calcite of burial origin (Fig. 6, Table 3; Glumac, 1997). Microbial micrite samples may have been contami-

nated by minor amounts of other carbonate components. However, given the careful sampling protocol, it is unlikely that their $\delta^{18}O$ values purely reflect contamination by non-marine components. Instead, the $\delta^{18}O$ values suggest that diagenetic modifications of microbial deposits most likely occurred as microscale, fabric-retentive recrystallization of micrite in the presence of meteoric and burial fluids. The more negative $\delta^{18}O$ values of microbial calcimicrite and most non-marine carbonate cements relative to non-microbial deposits (Fig. 6) suggest that the microbial deposits experienced more pronounced later diagenetic modifications than non-microbial calcimicritic deposits with diffuse burrows and rare intergranular pores. The difference in primary porosity, which is a direct function of the origin of microbial versus non-microbial deposits, may have played an important role in causing different diagenetic modification in these deposits.

Syndepositional growth cavities are a common feature of Early Cambrian microbial mounds (Rowland and Gangloff, 1988; Brasier et al., 1994; Whittaker et al., 1994), indicating the importance of early lithification in the formation of these deposits. However, the isotopic compositions of Lower Cambrian calcimicrobial carbonates tend to plot close to those of coeval non-microbial micrite-microspar carbonates (e.g., Brasier et al., 1994). Even though the evidence for the destruction of archaeocyathan and microbial mounds by borers dates back to the Early Cambrian (James et al., 1988; Rowland and Gangloff, 1988), common borings were not reported from the Lower Cambrian microbialites analyzed for their stable isotope compositions by Brasier et al. (1994). The additional porosity produced by the activity of borers may account for the isotopically altered compositions of the Upper Cambrian calcimicrobial carbonates from the southern Appalachians examined in this study. Oxygen isotope compositions of other examples of calcimicrobial carbonate need to be analyzed to determine if the proposed relationship between the extent of boring and the degree of later diagenetic alterations generally holds true.

Unlike the calcimicritic deposits, there is no difference between the $\delta^{18}O$ values of the non-microbial and microbial dolomicrite from the Upper Cambrian peritidal deposits in the southern Appalachians (Fig. 5; Table 1). Dolomitized microbial deposits formed by the trapping or agglutination of particles that were derived from the same source as the non-microbial dolomicrite. Dolomitized microbial and non-microbial deposits do not differ substantially in the type and amount of porosity; both have desiccation voids and evaporite molds filled with dolomite cement, and both have less common burrows with equant calcite cement. The microbial deposits also contain fenestrae, but they are fairly small, not interconnected, and were occluded during early diagenesis. Thus, dolomitized microbial and non-microbial deposits experienced very similar diagenetic histories. The fact that $\delta^{18}O$ values of peritidal dolomicrite, in general, are more positive than the $\delta^{18}O$ values of subtidal calcimicrite can be a consequence of: (1) an equilibrium fractionation between dolomite and calcite (Friedman and O'Neil, 1977); (2) the formation of dolomite under evaporative conditions (McKenzie, 1981); and (3) a lesser degree of diagenetic alteration of dolomite relative to calcite (Knoll et al., 1995).

The outcome of this study was quite surprising. It was predicted that the oxygen isotope values of shallow subtidal calcified microbialites would reflect most closely seawater composition (Glumac and Walker, 1997). Instead, the $\delta^{18}O$ values of these deposits were among the most negative values in the suite of samples analyzed. The results illustrate that the processes that promote early diagenetic calcification of microbialites also may influence late diagenesis and preferential alteration of these deposits, thus limiting the potential of ancient calcified microbial deposits for reconstructing geochemical signatures of syndepositional and early diagenetic conditions.

CONCLUSIONS

Upper Cambrian dolomicritic microbial deposits that formed by trapping or agglutination of particles do not differ substantially in their primary porosity from associated non-microbial dolomicrite and, consequently, these deposits experienced a similar diagenetic history. In contrast, early diagenetic lithification processes of cyanobacterial and bacterial calcification promoted the formation of growth cavities and borings, which served as conduits for fluids during later diagenesis of calcimicrobial deposits. This resulted in more pronounced diagenetic alterations of these deposits relative to the less porous, non-microbial deposits, as indicated by: (1) more negative $\delta^{18}O$ values of microbial calcimicrite in comparison with associated non-microbial calcimicrite; and (2) overlapping $\delta^{18}O$ values of microbial calcimicrite and non-marine carbonate cements.

ACKNOWLEDGMENTS

Graduate studies at The University of Tennessee, Knoxville (UTK), U.S.A., inspired my interest in diagenesis of microbial deposits. I thank K.R. Walker, A.J. Caldanaro, Jr., and the Carbonate Research Group members at UTK (1991–97) for their help and advice, and C.I. Mora and I. Richards for assistance with stable isotope analyses. J.D. Marshall, J. Andrews, I. Jarvis, and especially M.D. Brasier provided invaluable comments on an earlier version of this paper. This manuscript benefited greatly from critical reviews by two anonymous PALAIOS reviewers and from the prompt and professional handling by PALAIOS co-editors R.A. Gastaldo and C.E. Savrda.

REFERENCES

ANDREWS, J.E., CHRISTIDIS, S., and DENNIS, P.F., 1997, Assessing mineralogical and geochemical heterogeneity in the sub 63 micron size fraction of Holocene lime muds: Journal of Sedimentary Research, v. 67, p. 531–535.

BRASIER, M.D., 1993, Towards a carbon isotope stratigraphy of the Cambrian system: Potential of the Great Basin succession: *in* HAILWOOD, E.A., and KIDD, R.B., eds., High Resolution Stratigraphy: Geological Society of London, Special Publication 70, p. 341–359.

BRASIER, M.D., ROZANOV, A.Yu., ZHURAVLEV, A. Yu., CORFIELD, R.M., and DERRY, L.A., 1994, A carbon isotope reference scale for the Lower Cambrian succession in Siberia: Report of IGCP Project 303: Geological Magazine, v. 131, p. 767–783.

CHAFETZ, H.S., and BUCZYNSKI, C., 1992, Bacterially induced lithification of microbial mats: PALAIOS, v. 7, p. 277–293.

FAIRCHILD, I.J., MARSHALL, J.D., and BERTRAND-SARFATI, J., 1990, Stratigraphic shifts in carbon isotopes from Proterozoic stromatolitic carbonates (Mauritania): Influences of primary mineralogy and diagenesis: American Journal of Science, v. 290-A, p. 46–79.

FRIEDMAN, I., and O'NEIL, J.R., 1977, Compilation of stable isotope fractionation factors of geochemical interest: U.S. Geological Survey, Professional Paper 440-KK, p. 1–12.

GAO, G., and LAND, L.S., 1991, Geochemistry of Cambro-Ordovician Arbuckle limestone, Oklahoma: Implications for diagenetic $\delta^{18}O$ alteration and secular $\delta^{13}C$ and $^{87}Sr/^{86}Sr$ variation: Geochimica et Cosmochimica Acta, v. 55, p. 2911–2920.

GLUMAC, B., 1997, Cessation of Grand Cycle deposition in the framework of passive margin evolution: Controlling mechanisms and effects on carbonate deposition and diagenesis, Cambrian Maynardville Formation, southern Appalachians: Unpublished Ph.D. Dissertation, University of Tennessee, Knoxville, 380 p.

GLUMAC, B., and WALKER, K.R., 1997, Selective dolomitization of Cambrian microbial carbonate deposits: A key to mechanisms and environments of origin: PALAIOS, v. 12, p. 98–110.

GLUMAC, B., and WALKER, K.R., 1998, A Late Cambrian positive carbon-isotope excursion in the southern Appalachians: Relation to biostratigraphy, sequence stratigraphy, environments of deposition, and diagenesis: Journal of Sedimentary Research, v. 68, p. 1212–1222.

GLUMAC, B., and WALKER, K.R., 2000, Carbonate deposition and sequence stratigraphy of the terminal Cambrian grand cycle in the southern Appalachians: Journal of Sedimentary Research, v. 70, p. 952–963.

JAMES, N.P., KOBLUK, D.R., and KLAPPA, C.F., 1988, Early Cambrian patch reefs, southern Labrador: *in* GELDSETZER, H.H.J, JAMES, N.P., and TEBBUTT, G.E., eds., Reefs: Canada and adjacent areas: Canadian Society of Petroleum Geologists Memoir 13, p. 141–150.

KENNARD, J.M., and JAMES, N.P., 1986, Thrombolites and stromatolites: Two distinct types of microbial structures: PALAIOS, v. 1, p. 492–503.

KNOLL, A.H., KAUFMAN, A.J., and SEMIKHATOV, M.A., 1995, The carbon-isotopic composition of Proterozoic carbonates: Riphean successions from Northwestern Siberia (Anabar massif, Turukhansk uplift): American Journal of Science, v. 295, p. 823–850.

LOGAN, B.W., HOFFMAN, P., and GEBELEIN, C.D., 1974, Algal mats, cryptalgal fabrics and structures, Hamelin Pool, Western Australia: American Association of Petroleum Geologists Memoir 22, p. 140–194.

LOHMANN, K.C., and WALKER, J.C.G., 1989, The $\delta^{18}O$ record of Phanerozoic abiotic marine calcite cements: Geophysical Research Letters, v. 16, p. 319–322.

MCKENZIE, J.A., 1981, Holocene dolomitization of calcium carbonate sediments from the coastal sabkhas of Abu Dhabi, U.A.E.: A stable isotope study: Journal of Geology, v. 89, p. 185–198.

PATTERSON, W.P., and WALTER, L.M., 1994, Depletion of ^{13}C in seawater ΣCO_2 on modern carbonate platforms: Significance for the carbon isotopic record of carbonates: Geology, v. 22, p. 885–888.

PLAYFORD, P.E., and COCKBAIN, A.E., 1976, Modern algal stromatolites at Hamelin Pool, a hypersaline barred basin in Shark Bay, Western Australia: *in* WALTER, M.R., ed., Stromatolites: Developments in Sedimentology: Elsevier, Amsterdam, v. 20, p. 389–412.

PRATT, B.R., 1984, *Epiphyton* and *Renalcis*—Diagenetic microfossils from calcification of coccoid blue-green algae: Journal of Sedimentary Petrology, v. 54, p. 948–971.

REID, R.P., VISSCHER, P.T., DECHO, A.W., STOLZ, J.F., BEBOUT, B.M., DUPRAZ, C., MACINTYRE, I.G., PAERL, H.W., PINCKNEY, J.L., PRUFERT-BEBOUT, L., STEPPE, T.F., and DESMARAIS, D.J., 2000, The role of microbes in accretion, lamination and early lithification of modern marine stromatolites: Nature, v. 406, p. 989–992.

RIDING, R., 1975, *Girvanella* and other algae as depth indicators: Lethaia, v. 8, p. 173–179.

RIDING, R., 2000, Microbial carbonates: The geological record of calcified bacterial-algal mats and biofilms: Sedimentology, v. 47, Supplement 1, p. 179–214.

ROWLAND, S.M., and GANGLOFF, R.A., 1988, Structure and paleoecology of Lower Cambrian Reefs: PALAIOS, v. 3, p. 111–135.

SALTZMAN, M.R., RUNNEGAR, B., and LOHMANN, K.C., 1998, Carbon isotope stratigraphy of Upper Cambrian (Steptoean Stage) sequences of the eastern Great Basin: Record of a global oceanographic event: Geological Society of America Bulletin, v. 110, p. 285–297.

SURGE, D.M., SAVARESE, M., DODD, J.R., and LOHMANN, K.C., 1997, Carbon isotopic evidence for photosynthesis in Early Cambrian Oceans: Geology, v. 25, p. 503–506.

VISSCHER, P.T., REID, R.P., BEBOUT, B.M., HOEFT, S.E., MACINTYRE, I.G., and THOMPSON, J.A., 1998, Formation of lithified micritic laminae in modern marine stromatolites (Bahamas): The role of sulfur cycling: American Mineralogist, v. 83, p. 1482–1493.

WHITTAKER, S.G., JAMES, N.P., and KYSER, T.K., 1994, Geochemistry of synsedimentary cements in Early Cambrian reefs: Geochimica et Cosmochimica Acta, v. 58, p. 5567–5577.

ACCEPTED MAY 21, 2001